Optimal Connectivity during Multi-agent Consensus Dynamics via Model Predictive Control

Harikumar Kandath[1], Rajdeep Dutta[2], and J. Senthilnath[2]

Abstract— **In this paper, we solve an optimal consensus control problem of maximizing the state-dependent communication connectivity during a multi-agent consensus dynamics. A proportional-derivative type consensus controller is leveraged to drive agents into a symmetric formation. The asymptotic stability of the closed-loop system dynamics is established using Lyapunov theory, which helps us to deduce an intuitive time-varying gain profile based on a sufficient condition for convergence. Further, a Model Predictive Control approach is adopted to minimize a quadratic cost over a finite prediction horizon by adjusting the controller gains, such that the optimal connectivity is attained on the way with less control efforts, while handling constraints to agents' states, inputs, turn-rates and disturbances injected into agent velocities. Simulation results with time-varying controller gains demonstrate the impact of our proposed technique.**

I. INTRODUCTION

In automatic control and robotics research community, multi-agent systems (MAS) has been an active topic over the last decade due to its broad range of applications in distributed control, resource allocation and management, search and retrieval, surveillance and rescue operations, and target tracking and formation ([1], [2]). Cooperative agents in a dynamic fleet works efficiently upon attaining a general agreement among each other, i.e. consensus. The consensus control task becomes challenging to achieve when mobile agents are subjected to nonholonomic constraints. A group of nonholonomic mobile robots can be controlled distributively to reach a desired geometric pattern by driving the multi-agent graph's centroid along a specified trajectory [3]. Artificial potential fields have been exploited to stabilize the aggregate motion of a group of unicycles pursuing a position consensus [4]. In addition, the time-varying connectivity of an evolving MAS determines how well agents can communicate with each other during a mission, and renders controllability towards achieving a consensus objective ([2], [5]). To succeed in a cooperative mission, a multi-agent team needs to be connected throughout the dynamics [6].

In multi-agent cooperative control, connectivity maintenance and connectivity maximization are two distinct key problems. Maximizing connectivity makes agents more resilient to the environmental changes and improves the consensus convergence rather than only maintaining it [6], [7]. In [8], a decentralized control law was developed to drive a dynamic fleet along the connectivity supergradient direction to attain a final configuration with the highest connectivity. The authors in [9] addressed a combinatorial optimization problem of adding links to a graph from a set of candidates to maximize its algebraic connectivity, and proposed a heuristic based on the Fiedler vector to solve the underlying semi-definite program (SDP) with a standard convex relaxation. An iterative algorithm was proposed in [10] to solve a SDP problem involved in connectivity maximization, by finding the optimal vertex positional configuration. The authors in [11] considered a connectivity invariance problem, and designed a centralized protocol to control the structure of dynamic graphs such that the k-hop connectivity property is preserved under agent motions. Moreover, in [12], a flight routes addition/deletion problem was formulated and two algorithms, Modified Greedy Perturbation and Weighted Tabu Search, were proposed to enhance the weighted algebraic connectivity of the air transportation network by solving an associated relaxed SDP. Most of the existing research addressed MAS connectivity maximization as a standalone problem; however, the present work intends to maximize connectivity during a consensus dynamics. The main challenge arises due to the coupling between connectivity maximization and formation control, because the entire control effort can not be spent just to maximize the state-dependent connectivity of a dynamic MAS whose states are already driven by a consensus protocol.

In real-world dynamics, we must pay attention to how an agent responds to the environmental changes. For adaptive optimal control of constrained nonlinear systems, there exists model-free solution approach like adaptive dynamic programming (ADP) and model-based approaches such as control barrier function (CBF) and model predictive control (MPC). In distributed optimal consensus control problems [13], ADP can exploit additional compensators to circumvent the requirement of an original nonlinear system dynamics. Recently, authors in [14] leveraged CBF to maintain connectivity during the formation control of a constrained MAS. Also, Model Predictive Control (MPC) has been widely used in optimal control of dynamic multi-agent systems with constraints ([15], [16], [17]). An MPC approach has the potential to track a desired connectivity profile during the task of target-centric formation control [5]. In [18], another MPC method was exploited to generate optimal state trajectories for multi-agent consensus with single and double-integrator dynamics. Earlier research on optimal consensus by MPC, do not simultaneously account for consensus error, optimal connectivity, control effort and motion constraints in the respective formulations, which we address here.

[1] International Institute of Information Technology, Hyderabad-500032, India. Email: harikumar.k@iiit.ac.in.

[2]Department of Machine Intellection, Institute for Infocom Research, A*STAR, Singapore-138632. Email: rajdeep_dutta@i2r.a-star.edu.sg, Email: j_senthilnath@i2r.a-star.edu.sg

The contributions of this work are highlighted as follows: (a) Our proposed technique solves a challenging optimal control problem for steering cooperative agents into a position consensus with maximum connectivity on the way. (b) The adopted communication model is realistic as it accounts for state-dependent information exchange among agents. (c) The stability of the closed-loop system is established using Lyapunov theory, which unfolds an intuitive time-varying controller gain profile, i.e. stabilizing gain (SG). (d) While satisfying the stability criteria, we leverage MPC to adjust the controller gains with time such that maximum connectivity is attained by spending lower control efforts as compared to the SG-based control. (e) The proposed MPC approach handles constraints to agents' states, inputs, turn-rates, and random disturbances injected into the agent velocities.

The above contributions are validated with different case studies involving five agents with motion constraints. The rest of the paper is organized as follows. In Section II, we discuss the multi-agent communication model, and in Section III, we describe the associated motion model and consensus control along with the closed-loop stability analysis. Section IV illustrates our proposed MPC framework to achieve the optimal consensus. Simulation results are presented in Section V. Finally, Section VI concludes the present work.

II. COMMUNICATION MODEL

A dynamic MAS comprised of point-mass agents can be analyzed mathematically using a time-varying graph representation, $G_n(t) = (V, E(t))$, with V being a set of n nodes or agents and $E(t)$ being a set of variable number of edges or inter-agent connections [19]. Here, $G_n(t)$ is an undirected graph with bidirectional communication links.

Let, $\mathbf{x}_i \in \Re^{m\times 1}$ and $\mathbf{x}_j \in \Re^{m\times 1}$ denote the position state vectors of the i^{th} and the j^{th} agents, respectively; $\mathbf{r}_{ij} = \mathbf{x}_i - \mathbf{x}_j \in \Re^{m\times 1}$ denotes the relative displacement vector between agents $(i,\ j)$.

The time-varying connections among agents are captured by a state-dependent Laplacian matrix ([5], [8]), whose elements are given by

$$l_{ij}(t) = \begin{cases} -a_{ij}(t) & for\ i \neq j\ ; \\ \sum\limits_{j(\neq i)=1}^{n} a_{ij}(t) & for\ i = j\ , \end{cases} \tag{1}$$

where $a_{ij}(t) \neq 0$ only if $i \neq j$ and $j \in \mathscr{N}_i(t) = \{(j \neq i) \in V : \|\mathbf{r}_{ij}\| \leq R_u\}$; R_u in neighborhood $\mathscr{N}_i(t)$ denotes the communication range of agent i, which is consistent for all agents. The adjacency elements $a_{ij} = 1$ when $\|\mathbf{r}_{ij}\| \leq R_l$, and their magnitudes decay exponentially as inter-agent separations, $\|\mathbf{r}_{ij}\|$, increase from R_l to R_u, i.e. $a_{ij}(t) = exp(-\frac{\sigma(\|\mathbf{r}_{ij}\|-R_l)}{(R_u-R_l)})$; $\sigma > 0$ when $R_l \leq \|\mathbf{r}_{ij}\| \leq R_u$. Note that the Laplacian matrix, $L_n(t)$, is a positive semidefinite symmetric matrix. The second smallest eigenvalue of $L_n(t)$, i.e. $\lambda_2(t)$, is called the *Algebraic Connectivity* of the graph $G_n(t)$ [19], which quantifies the level of multi-agent communication at time t.

III. MOTION MODEL AND CONTROL

We consider a swarm of n agents with the kinematics of each agent governed by: $\dot{\mathbf{x}}_i(t) = [\dot{x}_i(t),\ \dot{y}_i(t)]^T = [v_{x_i}(t),\ v_{y_i}(t)]^T$, where $\mathbf{x}_i(t) = [x_i(t),\ y_i(t)]^T$ denotes the two-dimensional $(m = 2)$ position, $\mathbf{v}_i(t) = [v_{x_i}(t),\ v_{y_i}(t)]^T$ is the velocity vector and $\theta_i(t) = tan^{-1}(\frac{v_{y_i}(t)}{v_{x_i}(t)})$ is the heading angle of agent i at time t. The dynamics of agent i is given below.

$$\ddot{\mathbf{x}}_i(t) = [\dot{v}_{x_i}(t),\ \dot{v}_{y_i}(t)]^T = \mathbf{u}_i(t) \tag{2}$$

In (2), the control inputs to the i'th agent are its directional accelerations.

A. Consensus Controller

The traditional formation controllers work properly as long as there exists at least one spanning tree in the underlying multi-agent graph, which indicates $\lambda_2(t) > 0$. The task of achieving a position consensus can be formulated as a formation control objective given by: determine $\mathbf{u}_i(t)\ \forall\ i$ such that $(\hat{\mathbf{x}}_i(t) - \hat{\mathbf{x}}_j(t)) \to \mathbf{0}$ or $(\mathbf{x}_i(t) - \mathbf{x}_j(t)) \to (\mathbf{x}_{fi} - \mathbf{x}_{fj})$ as $t \to \infty$, where $\hat{\mathbf{x}}_i(t) = \mathbf{x}_i(t) - \mathbf{x}_{fi}$ represents the deviation of the current state $\mathbf{x}_i(t)$ of agent i from the desired final state $\mathbf{x}_{fi}$ for $j \in \mathscr{N}_i$. Rather than driving agents' absolute states, $\mathbf{u}_i(t)$ drives their evolving relative displacement vectors to the desired ones. A consensus protocol defines how agents must interact with each other in order to update their states. Here, we use a proportional-derivative type controller given by

$$\mathbf{u}_i = -\sum_{j\in\mathscr{N}_i} a_{ij}\{g_p(\hat{\mathbf{x}}_i - \hat{\mathbf{x}}_j) + g_v(\dot{\mathbf{x}}_i - \dot{\mathbf{x}}_j)\}\ , \tag{3}$$

where $\mathbf{u}_i = \ddot{\hat{\mathbf{x}}}_i(t) = \ddot{\mathbf{x}}_i(t) \in \Re^{m\times 1}$ is the acceleration control input applied to agent i while accessing the states of its neighbor(s) $j \in \mathscr{N}_i(t)$; $a_{ij}(t)$ is the time-varying weighting factor between the neighbors (i, j); and $g_p(t),\ g_v(t) > 0$ are the controller gains. Note that $g_v(t) > g_p(t)$ enforces moderate fluctuations in the multi-agent dynamics [5]. Equation (3) governs the dynamics of the i^{th} agent based on its neighborhood information. This equation can be extended for all agents using a matrix algebraic form as

$$\mathbf{U} = \ddot{\mathbf{X}} = -g_p(L_n \otimes I_m)\hat{\mathbf{X}} - g_v(L_n \otimes I_m)\dot{\mathbf{X}}\ , \tag{4}$$

where $\mathbf{X},\ \hat{\mathbf{X}},\ \mathbf{U} \in \Re^{mn\times 1}$; $\hat{\mathbf{X}}(t) = \mathbf{X}(t) - \mathbf{X}_f$ with $\mathbf{X}(t) = [\mathbf{x}_1(t)^T, \mathbf{x}_2(t)^T, ..., \mathbf{x}_n(t)^T]^T$ being the total agent state vector containing all member states at time t and $\mathbf{X}_f = [\mathbf{x}_{f1}^T, \mathbf{x}_{f2}^T, ..., \mathbf{x}_{fn}^T]^T$ being the total final position vector according to the desired symmetric formation; $\mathbf{U} = [\mathbf{u}_1^T, \mathbf{u}_2^T, ..., \mathbf{u}_n^T]^T$ is the total control input vector; $\otimes$ symbol stands for the Kronecker product, and $I_m \in \Re^{m\times m}$ denotes an identity matrix. The decentralized control law shown in (4), gives rise to a nonlinear system dynamics as follows.

$$\ddot{\hat{\mathbf{X}}} + g_v(L_n \otimes I_m)\dot{\hat{\mathbf{X}}} + g_p(L_n \otimes I_m)\hat{\mathbf{X}} = 0\ . \tag{5}$$

The coefficients in (5) are state-dependent, which reveals that the closed-loop system dynamics follows a nonlinear time-varying second-order differential equation.

B. Closed-loop Stability Analysis

The following presents the stability analysis of the closed-loop MAS under control input $\mathbf{U}$ (4), which is established using Lyapunov theory. First, let us consider a Lyapunov candidate function as follows.

$$V(t) = \frac{1}{2}\{\dot{\hat{\mathbf{X}}}(t)^T\dot{\hat{\mathbf{X}}}(t) + g_p(t)\hat{\mathbf{X}}(t)^T(L_n(t)\otimes I_m)\hat{\mathbf{X}}(t)\} \quad (6)$$

$V(t)$ in (6) is positive $\forall\ \hat{\mathbf{X}}$ except at $\hat{\mathbf{X}} = \eta \times \mathbf{1}_{nm}$ for $\eta \in \Re^1$, where $\mathbf{1}_{nm} \in \Re^{nm\times 1}$ represents the eigenvector of L_n corresponding to its 0 eigenvalue. By taking time-derivative on both sides of (6), we get

$$\begin{aligned}\dot{V}(t) &= \frac{1}{2}\times 2\ \dot{\hat{\mathbf{X}}}^T\ddot{\hat{\mathbf{X}}} + \\ &\quad + g_p\{\dot{\hat{\mathbf{X}}}^T(L_n\otimes I_m)\hat{\mathbf{X}} + \frac{1}{2}\hat{\mathbf{X}}^T(\dot{L}_n\otimes I_m)\hat{\mathbf{X}}\} + \frac{\dot{g}_p}{2}\hat{\mathbf{X}}^T(L_n\otimes I_m)\hat{\mathbf{X}} \\ &= \dot{\hat{\mathbf{X}}}^T\{\ddot{\hat{\mathbf{X}}} + g_p(L_n\otimes I_m)\hat{\mathbf{X}}\} + \frac{g_p}{2}\hat{\mathbf{X}}^T(\dot{L}_n\otimes I_m)\hat{\mathbf{X}} + \frac{\dot{g}_p}{2}\hat{\mathbf{X}}^T(L_n\otimes I_m)\hat{\mathbf{X}}\end{aligned} \quad (7)$$

We now substitute the closed loop MAS dynamics of (5) in (7), and obtain the following form of the Lyapunov candidate's time-derivative.

$$\dot{V}(t) = -g_v\dot{\hat{\mathbf{X}}}^T(L_n\otimes I_m)\dot{\hat{\mathbf{X}}} + \frac{g_p}{2}\hat{\mathbf{X}}^T(\dot{L}_n\otimes I_m)\hat{\mathbf{X}} + \frac{\dot{g}_p}{2}\hat{\mathbf{X}}^T(L_n\otimes I_m)\hat{\mathbf{X}} \quad (8)$$

$$\begin{aligned}&= -\begin{bmatrix}\dot{\hat{\mathbf{X}}}^T & \hat{\mathbf{X}}^T\end{bmatrix}\begin{bmatrix}g_v(L_n\otimes I_m) & \mathbf{0} \\ \mathbf{0} & -\frac{g_p}{2}(\dot{L}_n\otimes I_m) - \frac{\dot{g}_p}{2}(L_n\otimes I_m)\end{bmatrix}\begin{bmatrix}\dot{\hat{\mathbf{X}}} \\ \hat{\mathbf{X}}\end{bmatrix} \\ &\implies \dot{V}(t) = -\mathbf{Y}^T(L_{bl}\otimes I_m)\mathbf{Y}\ ,\end{aligned} \quad (9)$$

where $\mathbf{Y} = [\dot{\hat{\mathbf{X}}}^T,\ \hat{\mathbf{X}}^T]^T \in \Re^{2nm\times 1}$ and $L_{bl} \in \Re^{2n\times 2n}$ is composed of (g_vL_n) and $(-\frac{g_p}{2}\dot{L}_n - \frac{\dot{g}_p}{2}L_n)$ placed at its diagonal positions. The block diagonal matrix L_{bl} is positive definite when both of its constituent matrices are positive definite. g_vL_n is non-negative for $g_v > 0$, however, the concerning part is: $-(\frac{g_p}{2}\dot{L}_n + \frac{\dot{g}_p}{2}L_n)$. To guarantee the non-negativeness of L_{bl}, $(\frac{g_p}{2}\dot{L}_n + \frac{\dot{g}_p}{2}L_n)$ needs to be negative definite, which implies that the following relation holds for any real $\mathbf{v}_F$.

$$\mathbf{v}_F^T(g_p\dot{L}_n + \dot{g}_pL_n)\mathbf{v}_F < 0\ , \quad (10)$$

where $\mathbf{v}_F$ represents the Fiedler vector, which is the eigenvector of L_n corresponding to its second smallest eigenvalue, $\lambda_2 = \mathbf{v}_F^TL_n\mathbf{v}_F$. Since $L_n(t)$ is symmetric, the time-derivative of its eigenvalue can be expressed as [20]: $\dot{\lambda}_2(t) = \mathbf{v}_F^T(t)\dot{L}_n(t)\mathbf{v}_F(t)$. By substituting $\lambda_2 = \mathbf{v}_F^TL_n\mathbf{v}_F$ and $\dot{\lambda}_2 = \mathbf{v}_F^T\dot{L}_n\mathbf{v}_F$ into the inequality (10), we obtain

$$\begin{aligned}&g_p\dot{\lambda}_2 + \dot{g}_p\lambda_2 < 0 \ \text{ or, } \ \frac{\dot{\lambda}_2}{\lambda_2} + \frac{\dot{g}_p}{g_p} < 0 \\ &\text{or, } \ \frac{d}{dt}(\ln\lambda_2) + \frac{d}{dt}(\ln g_p) < 0\ , \quad (11) \\ &\implies d(\ln\lambda_2) + d(\ln g_p) = -c dt\ ;\ c > 0\ . \quad (12)\end{aligned}$$

Therefore, $\dot{V}(t) < 0$ can be ensured by satisfying the above inequality (11) with a proper selection of $g_p(t)$, obtained by solving (12), as follows.

$$g_p(t) = \frac{a}{\lambda_2(t)}e^{-ct}\ ;\ a, c > 0\ . \quad (13)$$

The solution gain profile in (13) reveals that $g_p(t)$ is inversely proportional with $\lambda_2(t)$ and tends to a constant value as $t \to 0$. Such a time-varying proportional gain profile is intuitive since it invests less control efforts as the team connectivity rises. To satisfy (11), it is sufficient for $g_p(t)$ to be bounded by: $g_p < \frac{a}{\lambda_2}$. The sufficient condition (13) ensures (10) that implies $\dot{V}(t) < 0$. Note that $V(t)$ decreases monotonically with time, indicating the potential of a gain design (13) towards maintaining $\lambda_2(t) > 0$ throughout if the initial and final configurations are connected.

In (8), both $\dot{L}_n$ and L_n have the common eigenvector $\mathbf{1}_{nm}$ corresponding to their zero eigenvalues. Hence, $\dot{V}(t) = 0$ occurs only at the invariance set: $\hat{\mathbf{X}} = \eta \times \mathbf{1}_{nm}$. Here, the constant η introduces an equal amount of translation to all agent positions, without affecting the pattern or symmetry of the multi-agent configuration. Thus, the asymptotic stability of the closed-loop system is ensured under a sufficient condition (11), i.e. $\hat{\mathbf{X}}(t) \to \eta \times \mathbf{1}_{nm}$ as $t \to 0$, which in turn means: $(L_n(t)\otimes I_m)\hat{\mathbf{X}}(t) \to \mathbf{0} \implies \mathbf{x}_i(t) - \mathbf{x}_j(t) \to \mathbf{x}_{fi} - \mathbf{x}_{fj}$.

The stability analysis gives us an intuitive gain selection scheme (SG) over time, under the assumption that every agent has perfect knowledge of the entire graph connectivity to evaluate the gains. Still, we are not sure how to adjust gains during a multi-agent dynamics such that maximum connectivity is attained without spending much control efforts while handling motion constraints. To seek the answer, we exploit model predictive control (MPC) with the fixed structure controller (4), as described below.

IV. Optimal Control via MPC

The *objective* is to maximize the state-dependent connectivity by utilizing least control efforts required from agents engaged in pursuing a position consensus.

By adjusting the controller gains over time, a MPC framework finds the optimal control sequence iteratively over a finite prediction horizon N_h. The discrete time state-space model for the second-order consensus dynamics (5) for a sampling interval of τ at the k^{th} instant, is given by

$$\begin{cases}\mathbf{X}(k+1) = \mathbf{X}(k) + \mathbf{V}(k)\tau + 0.5\mathbf{U}(k)\tau^2 \\ \mathbf{V}(k+1) = \mathbf{V}(k) + \mathbf{U}(k)\tau \\ \mathbf{U}(k) = -g_p(L_n(k)\otimes I_m)\hat{\mathbf{X}}(k) - g_v(L_n(k)\otimes I_m)\mathbf{V}(k)\ ,\end{cases} \quad (14)$$

where $\mathbf{X}(k)$, $\mathbf{V}(k)$, $\hat{\mathbf{X}}(k) \in \Re^{nm\times 1}$ denote the total position, velocity and deviation vectors at instant k. We now define the state and control input sequences: $\bar{\mathbf{Z}}(k) = \{\mathbf{Z}_k, \mathbf{Z}_{k+1}, ..., \mathbf{Z}_{k+N_h-1}\}$; $\mathbf{Z}(k) = [\mathbf{X}(k)^T, \mathbf{V}(k)^T]^T \in \Re^{2nm\times 1}$, and $\bar{\mathbf{U}}(k) = \{\mathbf{U}_k, \mathbf{U}_{k+1}, ..., \mathbf{U}_{k+N_h-1}\}$, respectively.

In our MPC formulation, the constrained optimization problem at decision instant k is given below.

$$\begin{aligned}&\underset{g_p(k),\ g_v(k)}{\text{minimize}} && J(\bar{\mathbf{Z}}(k), \bar{\mathbf{U}}(k)) \\ &\text{subject to} && c1: \mathbf{F}(k)[g_p(k),\ g_v(k)]^T \le \mathbf{H}(k) \\ &&& c2: \mathbf{Z}(k+1) = \mathbf{BM}(k)[g_p(k),\ g_v(k)]^T + \mathbf{AZ}(k) \\ &&& c3: 0 < g_p(k) < g_{pu} = \frac{a}{\lambda_2(k)},\ 0 < g_v(k) \le g_{vu}.\end{aligned} \quad (15)$$

The cost function $J(k)$ in (15) is computed as:

$$J(k)=\sum_{j=k}^{k+N_h-1}\left[Q(n_a-\lambda_2(j+1))^2+\mathbf{U}^T(j)\mathbf{R}\mathbf{U}(j)\right]\ , \quad (16)$$

where Q is a positive scalar and $\mathbf{R}$ is a constant positive definite matrix. The first and second quadratic terms in the right side of the expression (16) account for maximizing connectivity and lowering control effort, respectively.

The first constraint, $c1$, in the formulation (15) handles agents' velocity bounds: $\|v_i(k)\|_2 < v_b$, acceleration input bounds: $\|u_i(k)\|_2 < u_b$, and turn-rate limits: $|v_{xi}u_{yi}-v_{yi}u_{xi}| \leq \dot{\theta}_b\|v_i(k)\|_2^2$. Here,

$$\mathbf{F}(k)=[\mathbf{M}^T(k),\, -\mathbf{M}^T(k),\, \mathbf{M}^T(k)\tau,\, -\mathbf{M}^T(k)\tau,\, \mathbf{S},\, -\mathbf{S}]^T\ ,$$
$$\mathbf{H}(k)=[\frac{a_b}{\sqrt{2}}\mathbf{1}_{2nm}^T,\, \frac{v_b}{\sqrt{2}}\mathbf{1}_{nm}^T-\mathbf{V}^T(k),\, \frac{v_b}{\sqrt{2}}\mathbf{1}_{nm}^T+\mathbf{V}^T(k),\, \dot{\theta}_b\mathbf{1}_{2n}^T]^T\ ,$$

$\mathbf{M}(k) = -[(L_n(k)\otimes I_m)\hat{\mathbf{X}}(k),(L_n(k)\otimes I_m)\mathbf{V}(k)] \in \Re^{nm\times 2}$, $\mathbf{F}(k),\ \mathbf{H}(k)\in\Re^{(4nm+2n+1)\times 2}$, and $\mathbf{S}\in\Re^{2\times n}$ with its j^{th} column as:

$$\mathbf{S}_{:,j}=\frac{1}{||\mathbf{v}_j(k)||_2^2}[v_{xj}(k)\mathbf{M}_{2j,:}(k)-v_{yj}(k)\mathbf{M}_{2j-1,:}(k)]$$

$\forall j\in\{1,2,..,n\}$, where $\mathbf{M}_{j,:}(k)$ is the j^{th} row of $\mathbf{M}(k)$.

The second constraint, $c2$, in (15) enforces the optimization procedure to adhere to the system dynamics given in (14). Here,

$$\mathbf{A}=\begin{bmatrix} I_{nm} & \tau I_{nm}\\ 0_{nm} & I_{nm}\end{bmatrix}\in\Re^{2nm\times 2nm},\ \mathbf{B}=\begin{bmatrix}0.5\tau^2 I_{nm}\\ \tau I_{nm}\end{bmatrix}\in\Re^{2nm\times nm}\ .$$

The third constraint, $c3$, sets upper and lower bounds on the controller gains.

V. Numerical Evaluations

In simulations, we consider five agents with the second order dynamics given in (2). The sampling time τ is selected as 0.1 s; the bounds v_b and a_b are set as $10\sqrt{2}\ m/s$ and $2\sqrt{2}\ m/s^2$, respectively; the turn-rate is limited by $|\dot{\theta}_b|\leq 1.5\ rad/s$; the parameters R_l, R_u, σ of the communication model are selected as 10 m, 150 m, 5 m, respectively. The bounds on the control gains are: $g_{vu}=3$ and $g_{pu}(k)=\frac{1}{\lambda_2(k)}$. The optimization problem in (15) is solved by *fmincon* routine in MATLAB 2019b, with sequential quadrature programming (SQP) technique; parameters: $N_h=10,\ Q=100$, and $\mathbf{R}=I_{n\times n}$ (identity matrix). In the following, we present the numerical results for two different case studies.

In the first case study (Case I), the agents start from a low connectivity region ($\lambda_2\approx 0$) and move towards a high connectivity region ($\lambda_2=5$) to form a symmetric pentagon along the circumference of a circle of radius 5 m with an angular displacement of $\frac{2\pi}{5}$ rad between the adjacent agents. For the second case study (Case II), the agents start from a region of high connectivity ($\lambda_2\approx 4.2$) and move towards a low connectivity region ($\lambda_2\approx 1.7$) to form a symmetric formation along the circumference of a circle of radius 25 m. The initial positions (in m) and velocities (in m/s) of all the agents for both cases are shown in Table I. A performance comparison between the SG-based protocol (with $a=1$, $c=2\times 10^{-11}$) and the MPC-based protocol is presented in the following sections.

TABLE I: Initial positions and velocities of five agents.

Case	Agent	1	2	3	4	5
I	$x(0)\,(m)$	20	50	140	100	30
	$y(0)\,(m)$	140	120	10	130	30
II	$x(0)\,(m)$	2	5	14	10	3
	$y(0)\,(m)$	14	12	1	13	3
I & II	$v_x(0)\,(m/s)$	-0.63	-0.81	0.75	-0.83	-0.26
	$v_y(0)\,(m/s)$	0.80	0.44	-0.09	-0.92	-0.93

(Case I) Compact Formation: The connectivity profiles with MPC and SG are shown in Fig. 1a. The MPC is able to maintain a higher connectivity as compared to the SG. The average control effort defined by $\hat{\mathbf{U}}(k)=\frac{||\mathbf{U}^T(k)||_2}{n}$, is shown in Fig. 1b for MPC and SG. The RMS (root mean square) value of $\hat{\mathbf{U}}(k)$ is 1.648 m/s^2 and 2.288 m/s^2 for MPC and SG respectively. From Fig. 1a and Fig. 1b, it is clear that MPC raises the MAS connectivity better than SG by spending lower control effort. The corresponding control gain profiles are shown in Fig. 1c. The control effort is higher up to 10 s with the SG-based protocol as compared to the MPC-based protocol, since the former uses more g_p value than the latter. g_p for both MPC and SG become close to each other after around 10 seconds, resulting in almost equal control effort subsequently. The agent trajectories for MPC and SG are shown in Fig. 2. The desired symmetric formation is achieved by both MPC and SG. The total performance index associated with MPC, $PI=\sum_k J(k)$, decreases as the prediction horizon increases: $PI=9795.1,\ 9513.1,\ 9504.5$ for $N_h=10,\ 20,\ 30$, respectively.

The connectivity profile in the presence of a random velocity disturbance is shown in Fig. 3; this disturbance component is sampled from a uniform distribution and its maximum value lies within 20 % of an agent's maximum speed. The impact of the disturbance is negligible up to 20 sec as the agents move with high velocities, however, the same becomes prominent afterwards as the agents slow down while approaching the formation. The MPC based consensus reaches close to the desired connectivity faster as compared to the SG based consensus, with a lower control effort.

(Case II) Wide Formation: The resulting connectivity profiles with MPC and SG are shown in Fig. 4a. The MPC based connectivity profile reduces at a lower rate when compared to the SG based connectivity profile. The control efforts associated with MPC and SG are similar as shown in Fig. 4b. The corresponding control gain profiles are shown in Fig. 4c. The proportional gain, g_p, of MPC comes out to be lower than that of SG throughout time. The derivative gain, g_v, of MPC is initially lower than that of SG, however, they both become equal and constant after around 3 seconds. The agents reach the desired formation for both MPC and SG, as visible from their trajectories in Fig. 5.

VI. Conclusion

This research solves a nonlinear optimal consensus control problem for a MAS with second order dynamics by opti-

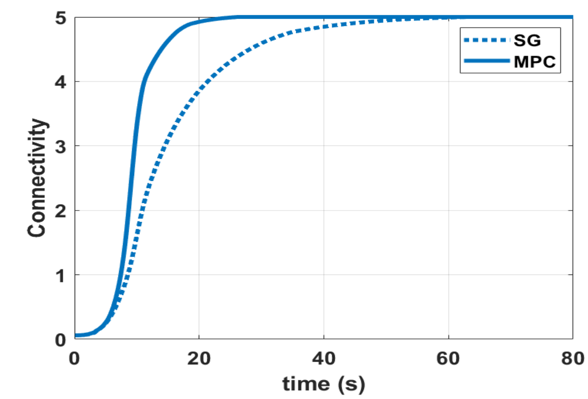

(a)

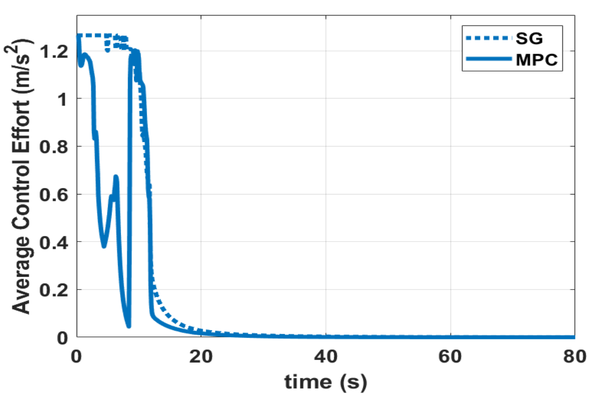

(b)

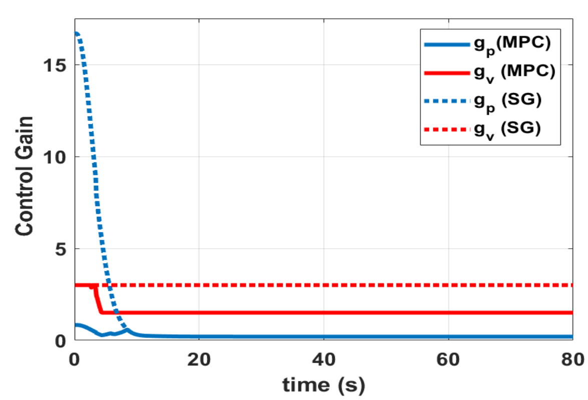

(c)

Fig. 1: Case I: (a) Connectivity profiles by MPC and SG (13); MPC maintains higher connectivity as compared to SG. (b) Average control effort profiles for MPC and SG. The RMS values are respectively 1.6480 m/s^2 (MPC) and 2.288 m/s^2 (SG). (c) Control gain profiles for MPC and SG.

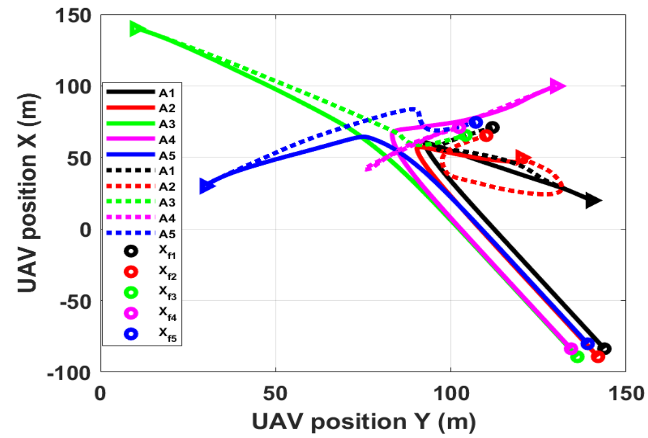

Fig. 2: Case I: 2D Trajectories (△ denotes the initial and ○ denotes the final locations) (a) MPC (b) SG

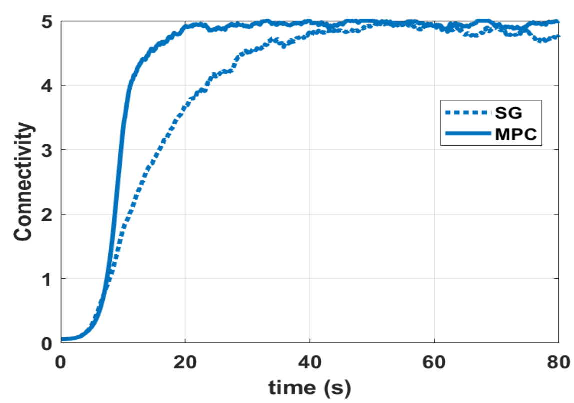

Fig. 3: Disturbance rejection (Case 1): Connectivity profiles by MPC and SG (13) with a velocity disturbance. The *RMS* values of average control effort are respectively 1.681 m/s^2 (MPC) and 2.374 m/s^2 (SG).

mally adjusting the control gains. The asymptotic stability of the nonlinear multi-agent consensus dynamics is established using Lyapunov theory, and an intuitive gain selection scheme (SG) is derived from the stability analysis. Moreover, the proposed MPC approach succeeds in determining time-varying gains to maximize the state-dependent connectivity with lower control efforts as compared to the SG-based control, while multiple cooperative agents pursue a position consensus. We further explored the potential of MPC to cope with the disturbances injected into agent velocities. In future, we plan to address more realistic aspects like intermittent communications among agents during formation control.

References

[1] W. Ren, R. W. Beard, and E. M. Atkins, "A survey of consensus problems in multi-agent coordination," in *Proceedings of the IEEE American Control Conference*. IEEE, 2005, pp. 1859–1864.

[2] W. Ren, "Multi-vehicle consensus with a time-varying reference state," *Systems & Control Letters*, vol. 56, pp. 474–483, 2007.

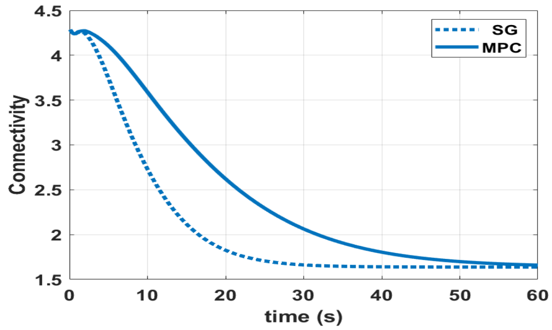

(a)

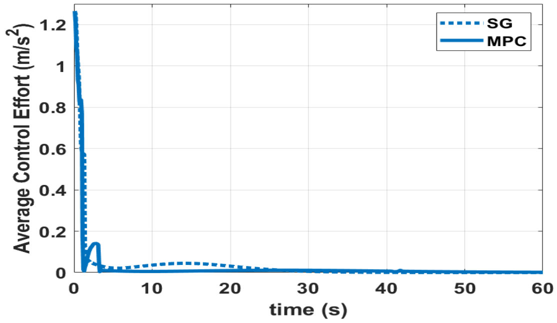

(b)

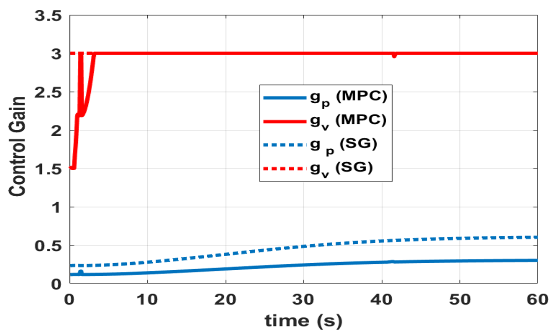

(c)

Fig. 4: Case II: (a) Connectivity profiles by MPC and SG; MPC gives higher connectivity than SG. (b) Average control effort by MPC is slightly less than SG with *RMS* values 0.6465 m/s^2 and 0.6757 m/s^2, respectively. (c) Control gain profiles by MPC and SG.

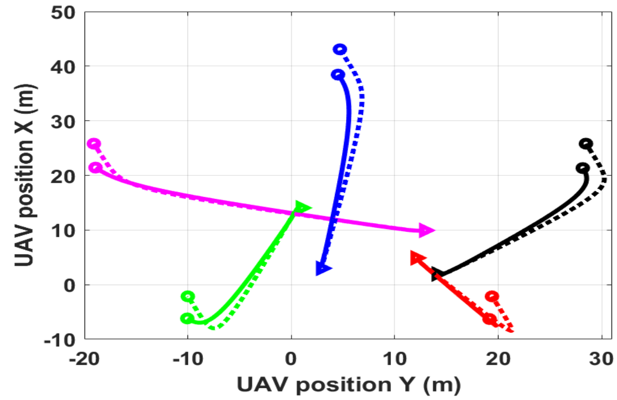

Fig. 5: Case II: 2D Trajectories (△ denotes the initial and ∘ denotes the final locations) by SG and MPC.

[3] Z. Peng, G. Wen, A. Rahmani, and Y. Tu, "Distributed consensus-based formation control for multiple nonholonomic mobile robots with a specified reference trajectory," *International Journal of Systems Science*, vol. 46, no. 8, pp. 1447–1457, 2015.

[4] K. D. Listmann, M. V. Masalawala, and J. Adamy, "Consensus for formation control of nonholonomic mobile robots," in *Proceedings of the IEEE international conference on robotics and automation*. IEEE, 2009, pp. 3886–3891.

[5] R. Dutta, L. Sun, and D. Pack, "Multi-agent formation control with maintaining and controlling network connectivity," in *Proceedings of the American Control Conference*. IEEE, 2016, pp. 1036–1041.

[6] K. Khateri, M. Pourgholi, M. Montazeri, and L. Sabattini, "A comparison between decentralized local and global methods for connectivity maintenance of multi-robot networks," *IEEE Robotics and Automation Letters*, vol. 4, no. 2, pp. 633–640, 2019.

[7] M. M. Zavlanos, M. B. Egerstedt, and G. J. Pappas, "Graph-theoretic connectivity control of mobile robot networks," *Proceedings of the IEEE*, vol. 99, no. 9, pp. 1525–1540, 2011.

[8] M. C. De Gennaro and A. Jadbabaie, "Decentralized control of connectivity for multi-agent systems," in *Proceedings of the 45th IEEE Conference on Decision and Control*. IEEE, 2006, pp. 3628–3633.

[9] A. Ghosh and S. Boyd, "Growing well-connected graphs," in *Proceedings of the 45th IEEE Conference on Decision and Control*. IEEE, 2006, pp. 6605–6611.

[10] Y. Kim and M. Mesbahi, "On maximizing the second smallest eigenvalue of a state-dependent graph laplacian," in *Proceedings of the American Control Conference*. IEEE, 2005, pp. 99–103.

[11] M. M. Zavlanos and G. J. Pappas, "Controlling connectivity of dynamic graphs," in *Proceedings of the 44th IEEE Conference on Decision and Control*. IEEE, 2005, pp. 6388–6393.

[12] P. Wei, L. Chen, and D. Sun, "Algebraic connectivity maximization of an air transportation network: The flight routes' addition/deletion problem," *Transportation Research Part E: Logistics and Transportation Review*, vol. 61, pp. 13–27, 2014.

[13] J. Zhang, H. Zhang, and T. Feng, "Distributed optimal consensus control for nonlinear multiagent system with unknown dynamic," *IEEE transactions on neural networks and learning systems*, vol. 29, no. 8, pp. 3339–3348, 2017.

[14] B. Capelli and L. Sabattini, "Connectivity maintenance: Global and optimized approach through control barrier functions," in *IEEE International Conference on Robotics and Automation*. IEEE, 2020, pp. 5590–5596.

[15] Q. Wang, Z. Duan, Y. Lv, Q. Wang, and G. Chen, "Distributed model predictive control for linear-quadratic performance and consensus state optimization of multiagent systems," *IEEE Transactions on Cybernetics*, 2020.

[16] J. Zhao and G.-P. Liu, "Time-variant consensus tracking control for networked planar multi-agent systems with non-holonomic constraints," *Journal of Systems Science and Complexity*, vol. 31, no. 2, pp. 396–418, 2018.

[17] C. E. Luis, M. Vukosavljev, and A. P. Schoellig, "Online trajectory generation with distributed model predictive control for multi-robot motion planning," *IEEE Robotics and Automation Letters*, vol. 5, no. 2, pp. 604–611, 2020.

[18] G. Ferrari-Trecate, L. Galbusera, M. P. E. Marciandi, and R. Scattolini, "Model predictive control schemes for consensus in multi-agent systems with single-and double-integrator dynamics," *IEEE Transactions on Automatic Control*, vol. 54, no. 11, pp. 2560–2572, 2009.

[19] C. Godsil and G. F. Royle, *Algebraic graph theory*. Springer Science & Business Media, 2013, vol. 207.

[20] J. R. Magnus, "On differentiating eigenvalues and eigenvectors," *Econometric theory*, vol. 1, no. 2, pp. 179–191, 1985.